

Photoacoustic spectrometer for measuring light absorption by aerosol: Instrument description.

W. Patrick Arnott, Hans Moosmüller, and C. Fred Rogers
Desert Research Institute
P.O. Box 60220
Reno NV 89506 USA

Tianfeng Jin and Reinhard Bruch
Physics Department
University of Nevada, Reno
Reno NV

Abstract

A photoacoustic spectrometer has been developed to measure *in situ* light absorption by aerosol. The measured quantity is the sound pressure produced in an acoustic resonator caused by light absorption. The current lower detection limit for light absorption is 0.4 Mm^{-1} which corresponds to an elemental carbon mass density of 40 ng/m^3 assuming an efficiency for light absorption of $10 \text{ m}^2/\text{g}$. Calibration is performed using simple theory for the instrument along with use of a calibrated microphone and laser. The acoustic resonator is operated in the plane wave mode, which has a quality factor of 80, a resonance frequency of 500 Hz, and a photoacoustic coefficient of $12.8 \text{ Pa (W m}^{-1})^{-1}$. The equivalent noise bandwidth of the resonator is 5 Hz. Coherent acoustic noise was suppressed through the use of acoustic notch filters and laser beam ports at pressure nodes of the resonator. The relatively low quality factor made it possible to use phase sensitive detection having an equivalent noise bandwidth of 7.5 mHz. This was achieved by vector time averaging the microphone signal for 8 minutes. Two compact, efficient lasers were used during instrument evaluation performed in the North Front Range Air Quality Study (Colorado, 1996/97). One was a laser diode pumped, frequency doubled, solid state laser, and the other was a laser diode. Laser wavelengths were 532 nm and 685 nm, and corresponding average powers were 60 mW and 87 mW. Some examples are provided for light absorption measurements using the photoacoustic instrument and a nearby aethalometer.

Key Words:

Light absorption, photoacoustic spectrometer, aethalometer, aerosol, elemental carbon, instrumentation.

Corresponding author:

W. Patrick Arnott
Tel.: 702-677-3123
Fax: 702-677-3157
e-mail: pat@sage.dri.edu

Introduction

We rely on fire in our daily lives, fire in our furnaces for heat, fire in our power plants for electricity, fire in our combustion engines to transport people and commodities. One of the prices we pay for our fires is air pollution and the generation of anthropogenic aerosol. A common type of aerosol that strongly absorbs visible light has a significant elemental carbon content, and is typically formed by incomplete combustion (Horvath, 1993). These aerosol negatively impact visibility (Horvath, 1993), are a health hazard when inhaled (Muir, 1995), may alter the global radiation balance and general circulation, and they also exist in the lower stratosphere (Pueschel et al., 1997).

A number of techniques have been devised to measure light absorption by aerosol. Many use the capture of aerosol on filters, followed by an optical measurement to determine aerosol light absorption. The aethalometer (Hansen et al., 1984) is a real time version of such an instrument. It may be desirable to measure aerosol light absorption by means that do not require the use of filters, and can observe the aerosol closer to its natural state. The photoacoustic technique is one method for doing this (Terhune and Anderson, 1977) and (Bruce and Pinnick, 1977). Electromagnetic energy absorbed by aerosol is converted to heat. Because the aerosol are small, and have sufficiently high thermal conductivity, the absorbed heat will flow rapidly to the surrounding air (Terhune and Anderson, 1977). Heated air responds by expanding its volume and/or pressure. By placing the aerosol laden air into an acoustic resonator, and modulating the electromagnetic power at its resonance frequency, the varying pressure disturbance (acoustic signal) can be amplified by the buildup of a standing acoustic wave in the resonator. Thus by

measuring the sound pressure that is associated with aerosol light absorption, a measure of elemental carbon concentration can be obtained.

A great many papers and several textbooks (Pao, 1977 and Rosencwaig, 1980) have extolled the virtues of photoacoustic spectroscopy for quantifying a wide assortment of material properties. This is a testament to the versatility and usefulness of the method. The reader is probably wondering what is new in our instrument. By taking advantage of technological innovation in laser efficiency and compactness, and applying photoacoustic ingenuity, we have built a useful photoacoustic spectrometer for aerosol light absorption measurement in most common field conditions. Our signal to noise limit is not currently limited by coherent acoustic noise caused mostly by window absorption of the modulated laser power. Therefore the sensitivity can be further improved by using higher laser power.

1. The photoacoustic spectrometer.

A schematic view of the photoacoustic spectrometer is shown in Figure 1. The principle of operation is as follows. The laser beam power is modulated at the acoustic resonance frequency of the photoacoustic spectrometer. Light absorbing components (gas or aerosol) convert laser beam power to an acoustic pressure wave through absorption induced gas expansion. A microphone detects the acoustic signal, and hence a measure of light absorption is produced. The piezoelectric disk is used to determine the acoustic resonance frequency of the spectrometer and the resonator quality factor (gain) to calibrate the system. Acoustic notch filters block most of the air-flow pump noise and spurious sound produced by absorption of light on the windows from entering the spectrometer. Holes for the laser beam (not shown) are placed at pressure nodes to minimize their coupling to the resonator mode. A somewhat similar

photoacoustic spectrometer has been previously discussed (Sigrist, 1994), though it does not use acoustic notch filters nor does it separate the windows from the resonator. Windows are placed directly at the pressure nodes.

Light absorption, B_{abs} , in dimensions of inverse distance, is determined from the acoustic pressure P_m , measured with the (calibrated) microphone and corrected for preamplifier gain; resonator quality factor Q ; resonance frequency f_0 ; the Fourier component of laser beam power P_L at f_0 ; and resonator cross sectional area A_{res} . The expression for B_{abs} is (Rosencwaig, 1980)

$$B_{\text{abs}} = P_m \frac{1}{P_L} \frac{A_{\text{res}}}{-1} \frac{2f_0}{Q}, \quad (1)$$

where $\gamma = 1.4$ is the ratio of isobaric and isochoric specific heats for air. Typical instrumental values were $P_L = 50$ mW to 105 mW (depending on the laser used), $A_{\text{res}} = 5.07$ cm², $f_0 = 500$ Hz, and $Q = 80$. The bandwidth of the photoacoustic spectrometer is approximately $f_0/(4Q) = 5$ Hz. The photoacoustic coefficient for the resonator from Eq. (1) is $P_m (P_L B_{\text{abs}})^{-1} = 12.8$ Pa (W m⁻¹)⁻¹. An example of measurement values for pressure were $P_m = 6$ μ Pa ($P_m = -10.5$ dB Rel. 20 μ Pa) that indicated light absorption $B_{\text{abs}} = 7.5$ Mm⁻¹. The broadband acoustic and electronic noise combined to produce a background level equivalent to $B_{\text{abs}} = 0.4$ Mm⁻¹ (to be discussed below).

A block diagram of the prototype photoacoustic spectrometer and detection electronics is shown in Fig. 2. A pump was used to draw outside air through the spectrometer with a volume flow rate of 3 L min⁻¹. Considering the volume of the spectrometer, this gives a flow rate time constant of about 8 sec. Acoustic notch filters were placed between the inlet and the spectrometer, and between the pump and the spectrometer to reduce the ambient and pump generated sound spectral energy at and near the resonance frequency of the spectrometer. These

are in addition to the filters on the spectrometer (Fig. 1). The laser power was modulated at the spectrometer acoustic resonance frequency using the square wave output of the waveform generator. The waveform generator provided timing for phase sensitive detection of the microphone signal by the lock-in amplifier and the Fast Fourier Transform (FFT) analyzer. The microphone signal was first amplified with a low noise preamplifier (typically by a factor of 100) and was band pass filtered (50 Hz bandwidth centered at 500 Hz). Preamplification was necessary to provide adequate signal level for the FFT analyzer. The FFT analyzer determined the magnitude of the Fourier component of acoustic pressure (P_m) at frequency f_0 . The FFT analyzer was also used to calibrate the spectrometer by issuing a single cycle of a sine wave to the piezo disk and obtaining the ratio (transfer function) of the spectral resonator response to the issued spectrum. The computer received the transfer function, and fit it to a standard resonance response function as a function of Q , f_0 , and the peak of the transfer function. The lock-in amplifier was used to determine the phase of the microphone signal relative to the waveform generator timing signal, and also determined the photodiode response at f_0 . The photodiode was calibrated with a laser power meter.

The entire measurement procedure was automated with use of the computer. The preamplifier communicated to the computer via a serial port. All other instruments were equipped with IEEE 488 communication capability. National Instruments Lab View software was used to provide a convenient user interface. Each measurement of light absorption was preceded with a resonator calibration using the FFT analyzer. The lock-in time constant was set to 10 seconds for light absorption measurements, and 128 averages lasting 4 seconds each were used with the FFT analyzer. The equivalent noise bandwidth of the FFT analyzer was 7.5

mHz. This measurement procedure gave photoacoustic spectrometer measurements of light absorption at 10 min intervals. Previous laboratory study indicated that the signal to noise ratio was proportional to the square root of the FFT analyzer total time of averaging, and was directly proportional to the laser power. The FFT analyzer should have been capable of measuring the relative phase between the microphone and waveform generator, though technical and time constraints prevented perfection of this measurement. The lock-in amplifier performed this task adequately. The preamplifier was not necessary for lock-in detection, though was used for convenience. A low pass filter setting of 24 dB per octave roll off was used on the lock-in amplifier.

The lasers used were both very compact and efficient:

- 532 nm doubled Nd:YAG laser diode pumped laser, 60 mW modulated average power.
- 685 nm laser diode, 87 mW modulated average power.

The 532 nm laser was only available for 2 days during the study (17 and 18 December 1996). The beam quality was excellent during this time. The 685 nm laser diode was confined to pass cleanly through the spectrometer only with the use of an initial collimating objective very near the diode followed by a cylindrical lens to circularize the beam, and finally followed by a convex lens to reduce the beam width. Square wave modulation was used for both lasers to maximize the Fourier component of light power at the resonance frequency. An infrared (802 nm wavelength) laser diode has previously been used for photoacoustic spectroscopy of carbon aerosol (Petzold and Niessner, 1992).

One consideration in selecting a laser wavelength for the photoacoustic spectrometer is to avoid gaseous atmospheric light absorption. If a gaseous absorption is due to a gas with constant

atmospheric concentration (e.g., O₂), a background signal is introduced. This background signal is only constant if the convolution of laser and gas spectrum is constant. The situation is worse if the concentration of the absorbing gas varies with time (e.g., H₂O). To select a wavelength with little gaseous absorption, atmospheric absorption coefficients B_{absg} have been calculated for the 1976 U.S. Standard Atmosphere (NASA, 1976) at sea level (T= 288 K, p=1013 mB, RH=46%) with a recent version (FASCOD3) of the Fast Atmospheric Signature Code (FASCODE) (Clough et al., 1981; Chetwynd et al., 1994). Three spectral regions of interest are shown in Fig. 3. The blue-green region (Fig. 3a) contains three laser lines of interest, the argon ion laser lines at 488.0 and 514.5 nm and the frequency doubled Nd:YAG laser line at 532.0 nm. The gaseous absorption coefficient is less than 0.1 Mm⁻¹ for both argon laser lines and less than 0.2 Mm⁻¹ for the Nd:YAG laser line. The red spectral region shown in Fig. 3b includes our red diode laser wavelength of 685 nm and the near infrared spectral region shown in Fig. 3c contains Petzold's and Niessner's diode laser wavelength of 802 nm. The absorption coefficient for a diode laser line cannot be specified as easily as for narrow band fixed frequency lasers. The diode laser center wavelength is a function of operating temperature (tuning coefficient = 0.3 nm K⁻¹), high power diode laser have a typical bandwidth of 2 nm, and their spectrum is commonly not well known. However, we have estimated the order of magnitude of the respective gaseous absorption by averaging the calculated absorption coefficients over a 2 nm interval centered on the nominal laser wavelength. This results in a gaseous absorption coefficient of ~ 0.1 Mm⁻¹ for our diode laser (685 nm) and of ~ 8 Mm⁻¹ for Petzold's and Niessner's diode laser (802 nm). Figure 2b also indicates that the 671 - 680 nm region is well suited for diode laser based measurement of aerosol light absorption with a gaseous continuum absorption coefficient around

0.1 Mm⁻¹ and no individual absorption lines. It should be kept in mind that these conclusion are only valid for the specified atmospheric composition. Especially high concentrations of ambient ozone (O₃) and nitrogen dioxide (NO₂) can increase gaseous absorption in the blue-green spectral region, while water vapor can have a similar effect in the red and near infrared region.

For our system, the copper metal design of the 1 m inlet tubing and the resonator proved to be quite efficient at removing NO₂ gas in laboratory evaluation using concentrations much higher than expected in field operation. This gas would normally be a strong source of light absorption at 532 nm and would have to be accounted for by other means if not removed. However, the cross section for absorption by NO₂ at 685 nm is negligible.

We can obtain the noise limit of the photoacoustic spectrometer in two ways. First, we simply place a filter over the inlet to the spectrometer to filter out essentially all aerosol, and record the resulting photoacoustic signal. The second technique allows us to simultaneously determine light absorption and an equivalent background noise level. The FFT analyzer spectral measurements away from the resonance frequency are first multiplied by a weighting function that increases the contribution of measurements farther away from resonance, and then an average of these values is obtained. The weighting function is the reciprocal of the standard resonance response function obtained from a curve fit of quality factor and resonance frequency which we determine during each calibration with the piezo disk. These measures of photoacoustic noise agree well, both in the laboratory and in the field, resulting in a noise limit of 0.4 Mm⁻¹.

2. Field evaluation of the photoacoustic spectrometer.

2a. The North Front Range Air Quality Study.

The Northern Front Range Air Quality Study (NFRAQS) is a major effort

- to determine the sources of air pollution in the Denver, Colorado, urban region, attributing to each source or source category an estimate of its emissions.
- to collect data necessary to support informed decisions leading to attainment of state visibility goals and federal air quality standards.

The winter intensive measurement period of NFRAQS extended from end of November 1996 to early February 1997. The 96/97 winter intensive of NFRAQS provided an ideal environment for the field evaluation of the DRI photoacoustic instrument at the Brighton, CO site.

Of particular relevance to the objectives of evaluating the photoacoustic spectrometer was the availability of colocated conventional measurements of aerosol scattering and absorption, taken with nephelometers and aethalometers, respectively. A full complement of aerosol filter measurements will also be available upon completion of the NFRAQS data analysis, and will be discussed in a second paper.

The Brighton site was located 20 miles northeast of downtown Denver. This semi-rural site provided an ideal opportunity to evaluate the photoacoustic spectrometer performance for both relatively clean (few light absorbing aerosol) and relatively dirty air. Relatively dirty air was often transported from Denver by wind from the southwest, and at other times, relatively clean air from rural areas was transported to the site when the winds were from the northeast. The site was located near the Brighton water towers, 1/4 mile east of town, and the photoacoustic system was housed in a small trailer used typically at construction sites. One initial concern was

the close proximity of high volume pumps, serving other measurements at the site, that produced a broadband acoustic background noise. We quickly determined that this noise source did not present a problem because the narrow band electronic detection and acoustic filters used in our instrument were sufficient.

2b. Comparison of photoacoustic spectrometer and aethalometer results.

The aethalometer determines light absorption based on deposition of aerosol on a quartz filter tape and subsequent light attenuation measurement of the loaded filter (Hansen et al., 1984). A constant factor is used to convert the filter attenuation measurement to an estimated light absorbing aerosol mass concentration in ng m^{-3} . To compare aethalometer and photoacoustic spectrometer measurements, the aethalometer mass concentration was multiplied by an assumed specific absorption efficiency of $10 \text{ m}^2 \text{ g}^{-1}$ to present the aethalometer data in the form of B_{abs} with dimensions of inverse distance. The photoacoustic spectrometer directly determines B_{abs} . The aethalometer wavelength is defined by a bandpass filter with a center wavelength of 530 nm, its flowrate was set to 5 L min^{-1} , and data were produced at 10 min intervals.

Photoacoustic spectrometer and aethalometer measurements of light absorption by aerosol for two 24 hour periods are shown in Fig. 4a and 4b. The temporal variation has been qualitatively connected with wind direction, with periods of higher B_{abs} related to wind from Denver and low B_{abs} related to wind from the relatively rural northeast Colorado. The 532 nm laser was used for the photoacoustic spectrometer results presented in Fig. 4a. The overall trends and magnitudes are generally very similar in Fig. 4a, though discrepancies near 04:00:00 are puzzling. The instruments were not evaluating the same air. They were in different trailers separated by 12 meters. The results in Fig. 4b show that the aethalometer measurements are

generally about a factor of 2 larger than the photoacoustic spectrometer results obtained with use of the 685 nm laser. Again the overall temporal trend is similar. The background photoacoustic noise, when processed to an equivalent light absorption signal, is slightly higher for the 532 nm data simply because the average power of this laser was about 0.7 times that of the 685 nm laser.

The wavelength dependence of light absorption by aerosol may help explain the discrepancy in Fig. 4b. Keep in mind that we have used a light absorption efficiency of $10 \text{ m}^2 \text{ g}^{-1}$ to express the aethalometer data originally in units of ng m^{-3} to units of Mm^{-1} . An efficiency of $3.1 \text{ m}^2 \text{ g}^{-1}$ for a wavelength of 802 nm has been determined (Petzold and Niessner, 1996), though a wide range of values can be found in the literature (Horvath, 1993). Iron oxide aerosol has about a factor of 4 greater absorption efficiency at a wavelength of 530 nm (aethalometer) compared with the efficiency at 685 nm (Ramsey-Bell, 1987), though it is not yet determined if this aerosol was present in high enough concentration to contribute significantly to total light absorption. Our comparison with aethalometer data suggests an efficiency of $5.4 \text{ m}^2 \text{ g}^{-1}$ for aerosol at 685 nm, though further evaluation with a larger data set will be discussed in a second paper.

Discussion.

The quality factor Q of the acoustic resonator is the amplification factor provided by the standing wave, as shown in Eq. (1). The Q is a ratio of the energy stored in the resonator to the acoustic energy dissipated per radian. A simple boundary layer approximation gives a theoretical value $Q \approx 80$, which agrees well with the observed value. This model takes into account thermal and viscous dissipation of the acoustic wave due to heat and momentum transfer at the curved and flat parts of the resonator interior. The dissipative volume is roughly the product of the

boundary layer thickness and the interior surface area, and the energy stored per cycle is related to the resonator interior volume. Thus Q is proportional to r , where r is the resonator radius. Because the resonator cross sectional area $A_{\text{res}} = r^2$, one implication of the photoacoustic equation, Eq. (1), is that the acoustic pressure generated is proportional to r^{-1} . Thus it seems that to make a photoacoustic spectrometer where a small absorption coefficient produces a large, easy to measure acoustic pressure, one should make the resonator radius as small as possible. However, practical considerations prevent use of very small resonator radii, and in our opinion, use of non-resonant photoacoustic techniques. We have found it very convenient to use a 2.54 cm microphone at one end of the resonator, and a similar sized piezoelectric disk for calibration at the other end. More important is the need to place holes in the resonator at pressure nodes to pass aerosol laden air and the laser beam through the resonator. By working with modest to high Q values, the traveling wave component at the resonant frequency is suppressed, so that flow noise and potential window absorption coherent noise produced near the pressure nodes do not couple well with the standing wave. Usually non-resonant photoacoustic spectrometers are operated at a considerably lower frequency than ours, and thus are more susceptible to the larger amount of electronic and acoustic noise generally present at lower frequency.

We recently have reported on a technique to control and increase resonator Q using a thermoacoustic method where properly placed thermoacoustic elements with a temperature gradient across them can provide acoustic power (rather than dissipation) to the standing wave in the resonator (Arnott et al., 1995). We showed that quality factors as high as $Q = 10,000$ could be achieved, and that the signal to noise ratio of the resonator alone is proportional to $Q^{1/2}$. However, the major disadvantage of such high Q techniques is that slight variations of the

resonance frequency with temperature and humidity cause a mismatch with the modulation frequency, making the system difficult to control for use with continuous wave lasers. We showed that long time averaging of the acoustic pressure with phase sensitive electronics provided by a lock-in amplifier or Fourier transform analyzer also greatly improves the signal to noise ratio (no surprise), and that use of modest resonator Q provided the highest overall signal to noise ratio because slight changes of the resonance frequency do not greatly alter the gain provided by the acoustic standing wave in the resonator. The high Q technique should be kept in mind, however, for applications that use a pulsed laser source where resonator Q stability is not the driving issue, and where nearly all noise suppression comes from the resonator alone (Brand et al., 1995).

While it is not the purpose of this paper to review previous efforts, some comparison of our system with previous efforts may be insightful. The Adams system (Adams et al., 1989) used an Argon ion laser with output power of 1 W. The detection limit of her system was $B_{\text{abs}} = 4.7 \text{ Mm}^{-1}$. Our lasers produced 50 mW to 100 mW output power, and used 3 orders of magnitude less electrical power than her system. The detection limit of our system was an order of magnitude better than her system, $B_{\text{abs}} = 0.4 \text{ Mm}^{-1}$, and we achieved this limit with 7% the laser power. Her detection limit was due to window absorption. Ours is currently not due to window absorption, but instead is due to acoustic and electronic noise. Increasing the laser power in our system should proportionally improve our detection limit. The eventual limit is determined by aerosol damage due to excessive laser irradiance.

A more recent European effort (Petzold and Niessner, 1996) yielded a system with a detection limit of $B_{\text{abs}} = 1.5 \text{ Mm}^{-1}$ that uses a 802 nm laser diode. The equivalent black carbon

concentration was estimated to be 500 ng m^{-3} . The drop off of aerosol absorption efficiency with increasing wavelength does not favor this wavelength, nor does the fact that you can not directly see the 802 nm beam so that alignment is more difficult. They used the 2nd azimuthal mode of a cylindrical resonator that operated at 6670 Hz with a quality factor of 300.

Acknowledgements.

Instrument development was supported by the U.S. Environmental Protection Agency, Office of Exploratory Research. Field evaluation was partially supported by this agency, and by the Desert Research Institute. We are grateful to Lincoln Sherman and Mitch Walker of the Atmospheric Resource Specialists, Inc. (Fort Collins, Colorado) and to John Walker (Pueblo, Colorado) for assistance with field operation and for providing preliminary aethalometer data. We are also grateful to David Dubois of the Desert Research Institute for the FASCODE calculations.

References

- Adams, K. M., L. I. Davis, Jr., S. M. Japar, and W. R. Pierson (1989). Real-Time, *In Situ* Measurement of Atmospheric Optical Absorption in the Visible via Photoacoustic Spectroscopy - II. Validation for Atmospheric Elemental Carbon Aerosol. *Atmospheric Environment* **23**, 693-700.
- Arnott, W. P., H. Moosmüller, R. E. Abbott, and M. D. Ossofsky (1995). Thermoacoustic Enhancement of Photoacoustic Spectroscopy: Theory and Measurements of the Signal to Noise Ratio. *Review of Scientific Instruments* **66**, 4827-4833.
- Brand, C., A. Winkler, P. Hess, A. Miklós, Z. Bozóki, and J. Sneider (1995). Pulsed-Laser Excitation of Acoustic Modes in Open High-Q Photoacoustic Resonators for Trace Gas Monitoring: Results for C₂H₄. *Applied Optics* **34**, 3257-3266.
- Bruce, C. W. and R. G. Pinnick (1977). In Situ measurements of light absorption with a resonant cw laser spectrophone. *Applied Optics* **16**, 1762-1765.
- Chetwynd, J. G., J. Wang, and G. P. Anderson (1994). FASCOD: An Update and Applications in Atmospheric Remote Sensing. *Proceedings SPIE* **2266**.
- Clough, S. A., F. X. Kneizys, L. S. Rothman, and W. O. Gallery (1981). Atmospheric Spectral Transmittance and Radiance: FASCOD1B. *Proceedings SPIE* **277**, 152-166.
- Hansen, A. D. A., H. Rosen, and T. Novakov (1984). The Aethalometer - An Instrument for the Real-Time Measurement of Optical Absorption by Aerosol Particles. *Science of the Total Environment* **36**, 191-196.
- Horvath, H. (1993). Atmospheric Light Absorption - A Review. *Atmospheric Environment* **27A**, 293-317.
- NASA (1976). *U.S. Standard Atmosphere Supplements*. U. S. Government Printing Office, Washington, D.C.
- Pao, Y.-H. (1977). *Optoacoustic Spectroscopy and Detection*. Academic Press, New York, NY.
- Petzold, A. and R. Niessner (1992). In Situ measurements on carbon aerosols with photoacoustic spectroscopy. *SPIE Proc.* **1716**, 510-516.
- Petzold, A. and R. Niessner (1996). Photoacoustic Soot Sensor for *in-Situ* Black Carbon Monitoring. *Applied Physics* **B 63**, 191-197.
- Pueschel, R. F., K. A. Boering, S. Verma, S. D. Howard, G. V. Ferry, J. Goodman, D. A. Allen, and P. Hamill (1997). Soot aerosol in the lower stratosphere: Pole-to-pole variability and contributions by aircraft. *Journal of Geophysical Research* **102**, 13113-13118.
- Ramsey-Bell, D. C. (1987). Photoacoustic measurements of atmospheric aerosol absorption coefficients at ultraviolet, visible, and infrared wavelengths. Dissertation, University of Arizona, 155.
- Rosencwaig, A. (1980). *Photoacoustics and Photoacoustic Spectroscopy*. Wiley, New York, NY.
- Sigrist, M. W. (1994). "Air Monitoring by Laser Photoacoustic Spectroscopy." In *Air Monitoring by Spectroscopic Techniques*, M. W. Sigrist (Ed.) Wiley, New York, **127**, 186.
- Terhune, R. W. and J. E. Anderson (1977). Spectrophone Measurements of the Absorption of Visible Light by Aerosols in the Atmosphere. *Optics Letters* **1**, 70-72.

FIGURE CAPTIONS

Figure 1. Schematic view of the prototype photoacoustic spectrometer.

Figure 2. Block diagram of the prototype photoacoustic spectrometer, detection electronics, and air sampling arrangement. The computer was interfaced with all of the detection electronics (not shown).

Figure 3. FASCODE atmospheric absorption spectra in the (a) blue-green, (b) red, and (c) near infrared regions.

Figure 4. Typical comparison of aethalometer and photoacoustic spectrometer determinations of light absorption by aerosol during NFRAQS. In a), the 532 nm laser was used for the photoacoustic spectrometer, though the 685 nm laser was used in b).

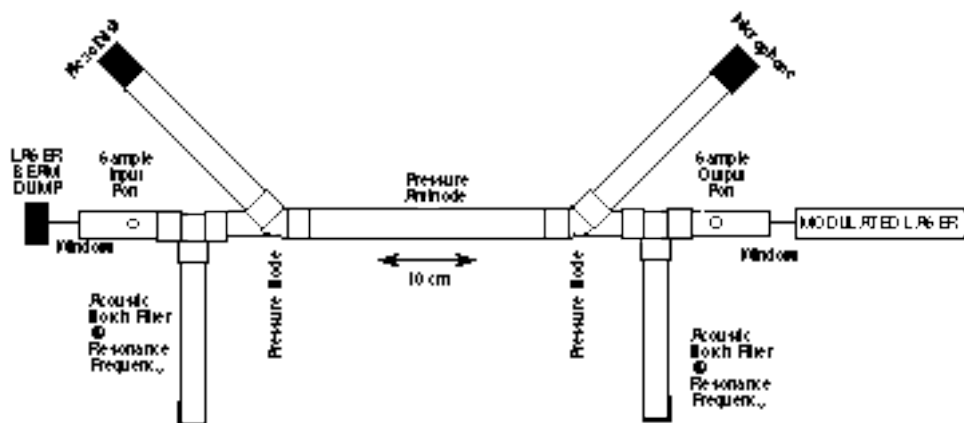


Figure 1. Schematic view of the prototype photoacoustic spectrometer.

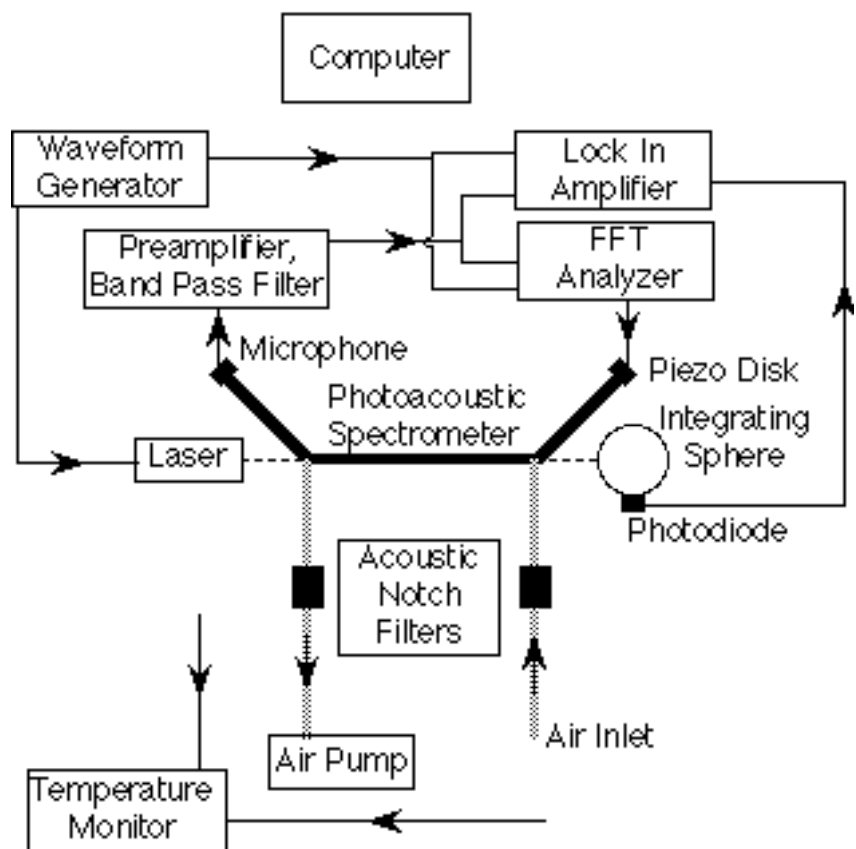


Figure 2. Block diagram of the prototype photoacoustic spectrometer, detection electronics, and air sampling arrangement. The computer was interfaced with all of the detection electronics (not shown).

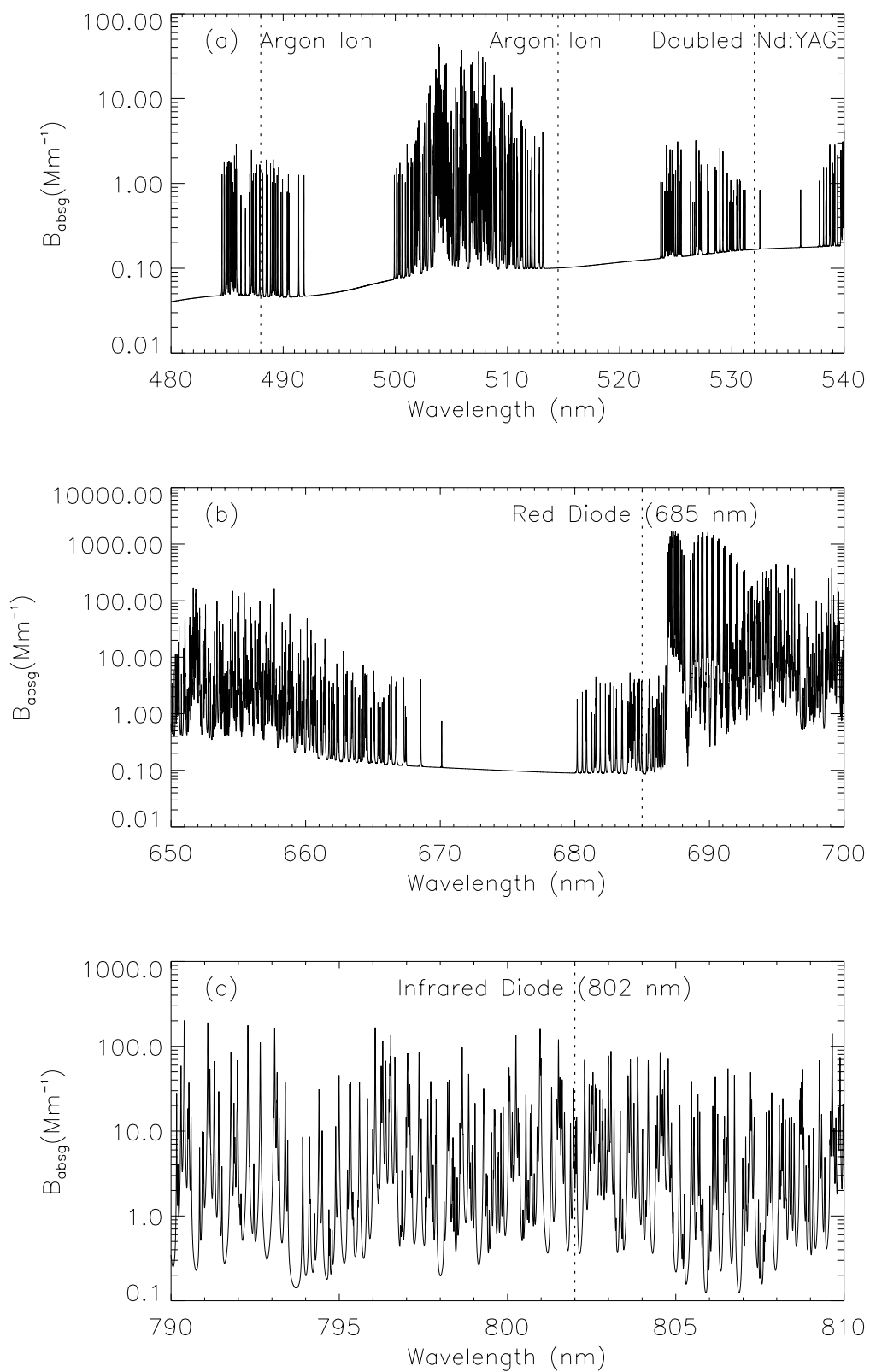


Figure 3. FASCODE atmospheric absorption spectra in the (a) blue-green, (b) red, and (c) near infrared regions

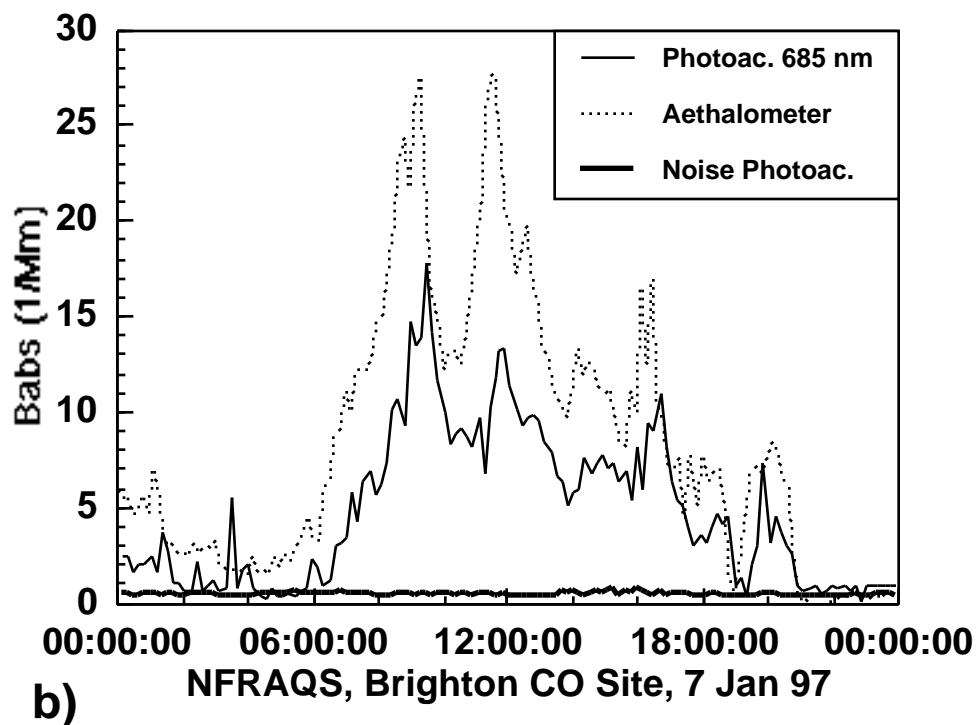
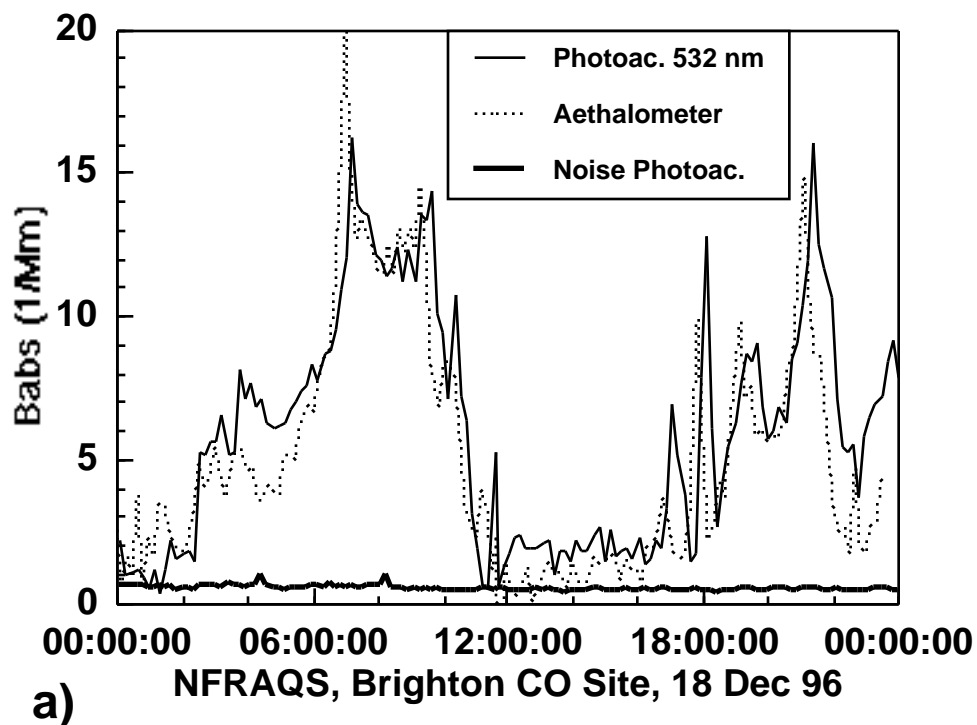


Figure 4. Typical comparison of aethalometer and photoacoustic spectrometer determinations of light absorption by aerosol during NFRAQS. In a), the 532 nm laser was used for the photoacoustic spectrometer, though the 685 nm laser was used in b). Thick solid curves are the estimated background noise.